

We are IntechOpen, the world's leading publisher of Open Access books Built by scientists, for scientists

6,900

Open access books available

185,000

International authors and editors

200M

Downloads

Our authors are among the

154

Countries delivered to

TOP 1%

most cited scientists

12.2%

Contributors from top 500 universities



WEB OF SCIENCE™

Selection of our books indexed in the Book Citation Index
in Web of Science™ Core Collection (BKCI)

Interested in publishing with us?
Contact book.department@intechopen.com

Numbers displayed above are based on latest data collected.
For more information visit www.intechopen.com



Surfactant Transfer in Multiphase Liquid Systems under Conditions of Weak Gravitational Convection

Konstantin Kostarev¹, Andrew Shmyrov¹,
Andrew Zuev¹ and Antonio Viviani²

¹*Institute of Continuous Media Mechanics,*

²*Seconda Università di Napoli*

¹*Russia,*

²*Italy*

1. Introduction

To day, investigation of mass transfer between a drop and a surrounding medium is one of the most promising and at the same time the most complicated fields of research. The relevance of these investigations should be attributed to the fact that drops participate in many technological processes including extraction, mixing, dissolution, etc. The complexity of studies is caused by small dimensions and spherical shape of the drops which severely restricts the possibilities of experimental investigation (Henschke & Pfennig, 1999; Agble & Mendes-Tatsis, 2000; Kosvintsev & Reshetnikov, 2001; Amar *et al.*, 2005; Waheed *et al.*, 2002). As a result the majority of studies into the process of mass transfer between a drop and an ambient fluid cover theoretical aspects of the problem and are based on different simplifications and assumptions on the character and the level of interaction between mass transfer mechanisms (Myshkis. *et al.*, 1987; Subramanian *et al.*, 2001; Bratukhin *et al.*, 2001). Therefore the results of these studies require experimental verification especially in the case of surfactant diffusion, which can locally change the surface tension at the interface and initiate the solutocapillary motion even in initially homogeneous solutions (Wegener *et al.*, 2007, 2009a, 2009b; Burghoff & Kenig, 2006).

The character of interaction between buoyancy and capillary convections generally strongly depends on the gravity level. At most times it is suggested that the buoyancy plays the main role under normal gravity and that the capillary forces dominate in microgravity conditions. However at normal gravity conditions the free convection motion provides conditions for recovering the percentage composition of the liquid mixtures near the interface. With reduction in the gravity level the outflow of both the diffusing component and depleted mixture decreases. Lowering of the concentration gradient normal to the interface reduces the probability of formation of the concentration inhomogeneities along this boundary. Therefore the possibility for the occurrence of solutocapillary motion during mass transfer processes under microgravity conditions is still an open question.

In the autumn of 2007 the space experiment "Diffusion of a surfactant from a drop" was carried out during the orbital flight of the spacecraft Foton-M3 (Kostarev *et al.*, 2010). The performed experiment was aimed at studying the development of the capillary convection

during surfactant diffusion. In the framework of terrestrial simulation of the next space experiment we carried out a series of laboratory tests to provide insight into the nature of surfactant transfer from the liquid to the drop in a thin horizontal layer. The main results of our space and terrestrial investigations of mass transfer between a drop and a surrounding medium are presented below.

2. Experimental apparatus and technique

In terrestrial simulation of microgravity conditions the use of the horizontal liquid layer of small thickness gave us twofold benefits. First, it allowed a maximum reduction of intensity of the gravitational flow and second it allowed us to use a specific experimental technique – generation of a drop in the form of a short and wide vertical cylinder. The drop is bounded at the top and the bottom by the solid surfaces and has a free lateral surface which offers new possibilities for visualization of the surfactant distribution inside and outside the drop by means of optical methods. During laboratory experiments we investigated diffusion of isopropyl alcohol (used as a surfactant) from the drop of its mixture with chlorobenzene to the surrounding water (section 3, dissolving drop) or contrariwise from its ambient aqueous solution to the drop of chlorobenzene (section 5, absorbing drop). The isopropyl alcohol is lighter than water, which, in turn, has a lower density than chlorobenzene. All fluids and their solutions used in tests were transparent. The isopropyl alcohol is well soluble both in water and chlorobenzene, although the magnitudes of its solubility in these fluids differ essentially. In particular, an equilibrium distribution of alcohol between the solution and the drop is reached when its concentration in water C_0 and chlorobenzene C_d is 10% and 1.2%, respectively (Fig. 1). The limiting solubility of pure chlorobenzene in water is as low as 0.05% at 30°C and that of water in chlorobenzene is even lower. However, the reciprocal solubility of these two fluids increases with a growth of alcohol concentration in both fluids. Therefore, at low surfactant concentrations the absorbing drop during mass transfer adds only one component of the mixture – alcohol, whereas at high concentrations we might expect generation of appreciable counter-flows of the base fluids.

Visualization of the surfactant distribution was made with the help of the Fizeau interferometer (Gustafson *et al.*, 1968; Kostarev & Pshenichnikov, 2004). In accordance with the goals of experiment the interferometer was subjected to modernization, which consisted in creation of an additional unit including mirror 9 tilted at an angle of 45° to the laser beam axis, cuvette with a horizontal fluid layer 6 and video camera 8 to record the transmitted-light image of the drop (Fig. 2). The axis of rotation of the unit coincided with the optical axis of the parallel beam formed by collimator 5 of the interferometer. The center of the mirror and the beam axis also coincided in such a way that the laser beam was perpendicular to the plane layer containing the drop at any orientation of the cuvette with respect to the vector of the gravitational force. The selected scheme of the experimental setup enabled us to control the intensity of the gravitational action by way of changing the angle of inclination of the plane layer. However it also required an additional adjustment for horizontal positioning of the layer achieved with the error of less than 30''.

The interferometer cell in the form of rectangular parallelepiped 1.2 mm thick, 90 mm length and 50 mm width was used to create an element of an infinite thin horizontal layer. The surfactant distribution in the liquid layer inside the cell was visualized on its wide side. In the isothermal case the results of visualization of the concentration inhomogeneities in the fluid solutions were obtained as a system of interference bands, representing isolines of equal optical path length. In case of the mixture composition varies only across the

transmitted light beam the interference bands could be identified with certain values of the surfactant concentration. Thus, for the layer 1.2 mm thick a transition from one band to another corresponded to a variation in the alcohol content in water from 0.27% at $C_0 = 5\%$ to 0.81% at $C_0 = 45\%$ (Zuev & Kostarev, 2006). For the chlorobenzene mixture a similar transition occurred due to a change in the alcohol concentration by 0.10%. The initial diameter D_0 of the cylindrical drops injected into the liquid layer with a medical syringe varied from 3 to 9 mm. The ambient temperature of experiments was $(23\pm1)^\circ\text{C}$.

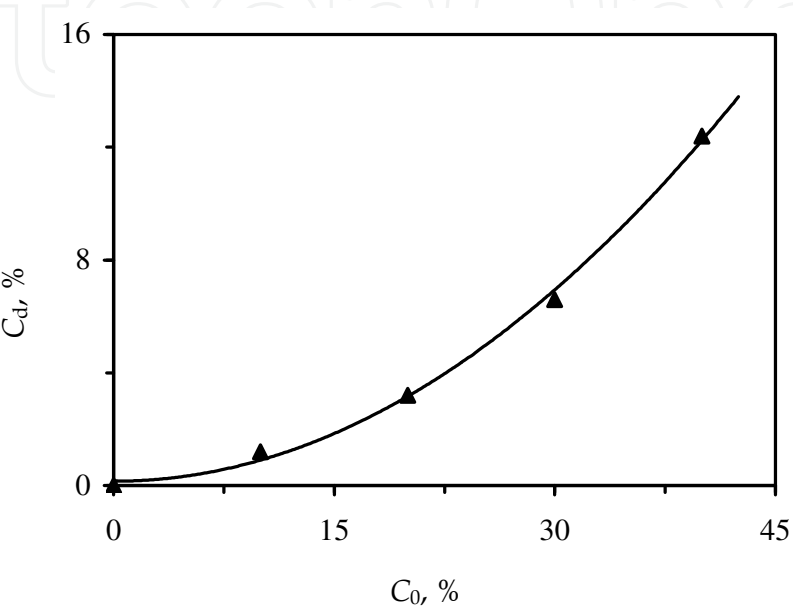


Fig. 1. Equilibrium concentration of isopropyl alcohol in the drop versus its concentration in the surrounding solution

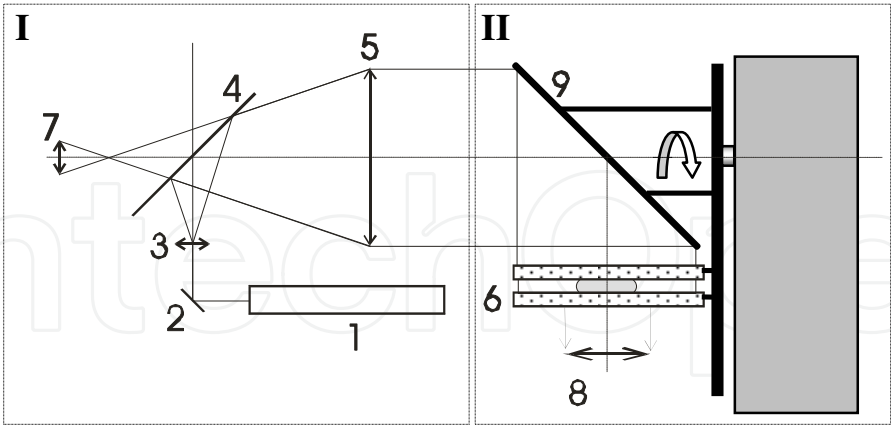


Fig. 2. Schematics of the experimental setup: 1 – laser; 2 – rotating mirror; 3 – micro-lens; 4 – semi-transparent mirror; 5 – lens-collimator; 6 – plane layer with a drop; 7 and 8 – video cameras, 9 – tilting mirror

3. Surfactant diffusion from drop (terrestrial simulation)

For investigation of surfactant dissolution process we used the chlorobenzene drops with the initial mass concentration of the isopropyl alcohol C_d ranged from 1% to 20%. A typical

series of interferograms of the concentration field generated around a dissolving drop of the mixture containing surfactant is shown in Fig. 3. It is seen that the process of surfactant diffusion begins concurrently with the formation of the drop (Fig. 3,a) and even earlier and has three-dimensional character despite a small thickness of the layer and its horizontal position. The alcohol, escaping from the drop, did not have time to mix with water due to a low diffusion and therefore it floated up forming a thin layer along the upper boundary of the cell. A similar situation could be observed inside the drop – chlorobenzene, which had already got rid of the alcohol, sank along the lateral walls of the drop and moved along the bottom towards its center. As a result, vertical gradients of the surfactant concentration were formed both in the drop and in the layer. Capillary convection occurred practically immediately after formation of the drop. It developed in the form of three-dimensional nonstationary cells symmetrically formed at both sides of the interface. In a short time the size of the cells became comparable with the drop radius, which provided conditions for a rapid decrease of the surfactant concentration due to a continuing transfer of the mixture from the central region of the drop to the interface. Note that the capillary flow had a rather weak effect on the gravitational flow responsible for the propagation of the concentration front in a direction away from the drop boundary (such level of the interaction manifests itself in a dramatic distinction between two types of the convective motion shown in Fig. 3,b). At the same time, the boundary of the concentration front had still the traces of the originating cell flow (Figs. 3,b–3,d).

A decrease of the surfactant content in the drop smoothed down the concentration differences at the interface and the capillary flow decayed. After this the evolution of the concentration field was governed solely by the buoyancy force, which essentially simplified its structure (Fig. 3,c). As long as the amount of surfactant in the drop remained rather high, regeneration of the vertical solutal stratification at the interface led again to the development of the intensive capillary convection (Fig. 3,d). However, the arising cell motion continued for no more than a few seconds and was followed by the gravitational flow with essentially lower characteristic velocities. Depending on the initial surfactant concentration the number of such "outbursts" of the capillary convection could vary in the range from one or two at $C_d = 5\%$ to eight at $C_d = 20\%$ (it is to be noted that the number of outbursts markedly varied from test to test at the same value of C_d). The period of the alternation of different convective flow patterns was rather short (it lasted approximately two minutes at $C_d = 20\%$ for a drop with $D_0 = 5.6$ mm). Completion of the surfactant dissolution from the drop proceeded under conditions of quasi-diffusion. Depending on the values of C_d and D_0 the time of full dissolution varied from 7 to 10 minutes, which was tens times shorter than the characteristic times of diffusion.

At described series of interferograms the transmitted beam passed through the optical medium, whose properties were changing along direction of the light propagation. This rendered the interpretation of the current interference pattern impossible (because in the considered situation it was the main source of information concerning the two unknown quantities – the amount and extent of the concentration inhomogeneity). On the other hand, the visualized distribution of the isolines of equal optical path length was formed by the field of surfactant concentration which enabled us to watch its propagation throughout the cell volume, to estimate the intensity of its variation using the rate of change of the interference bands at the selected points (e.g. in drop center) and also to define the characteristic times of the main stages of the dissolution process (Kostarev *et al.*, 2007).

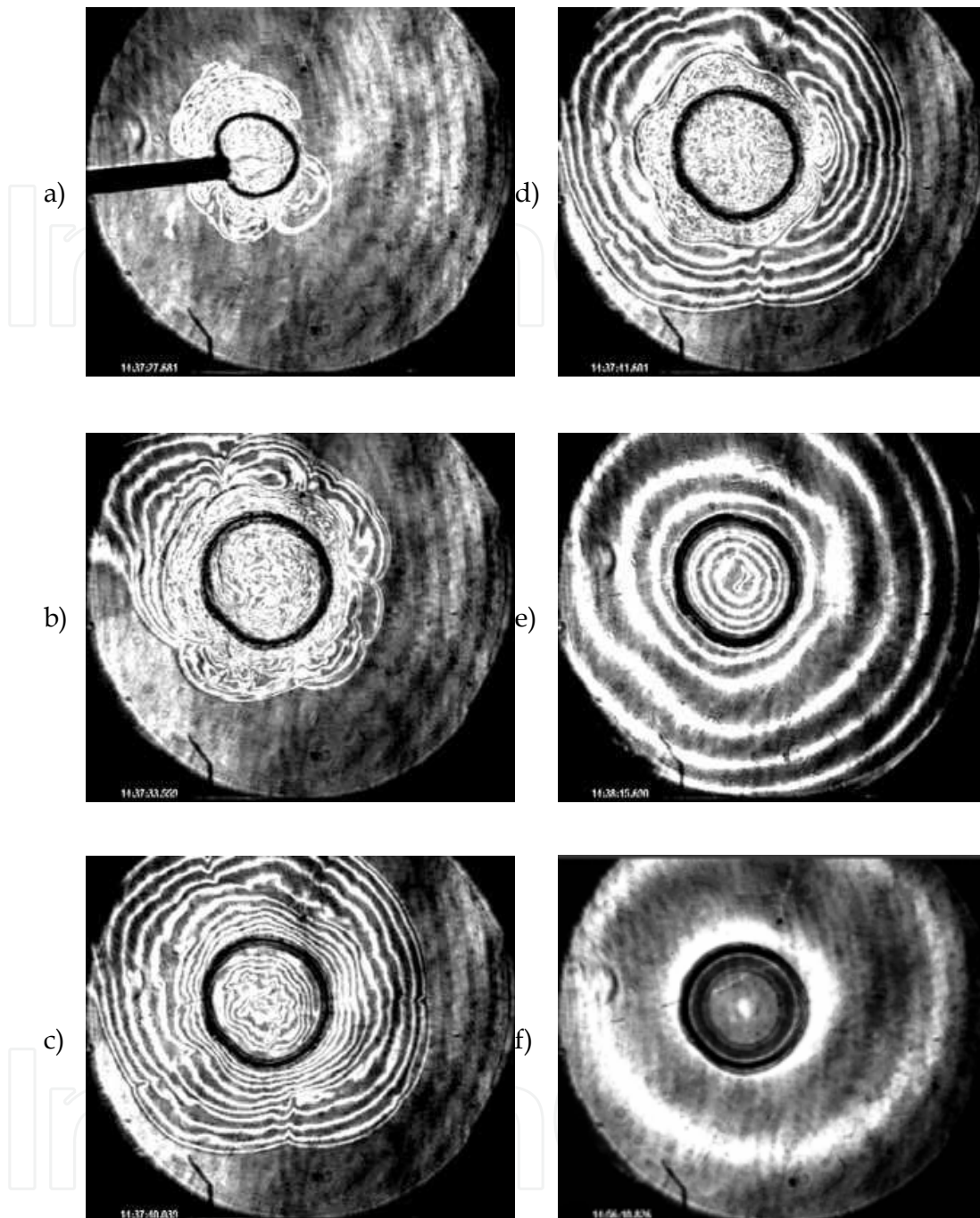


Fig. 3. Distribution of concentration during dissolution of the alcohol from the drop. $D_0 = 4.7$ mm with $C_d = 15\%$ in a horizontal layer 1.2 mm thick. t , sec: 1 (a), 7 (b), 13 (c), 15 (d), 49 (e), 580 (f)

In view of the fact that on the interferogram a transition from one interference band to another cannot be correlated with a certain variation of the concentration value, the relationships describing evolution of the concentration field will be presented without revaluation, i.e. as time variation of the number of interference bands N at the selected points. However we propose to retain the term "distribution of concentration" for discussion of the visualization results bearing yet in mind that the field structure is three-dimensional.

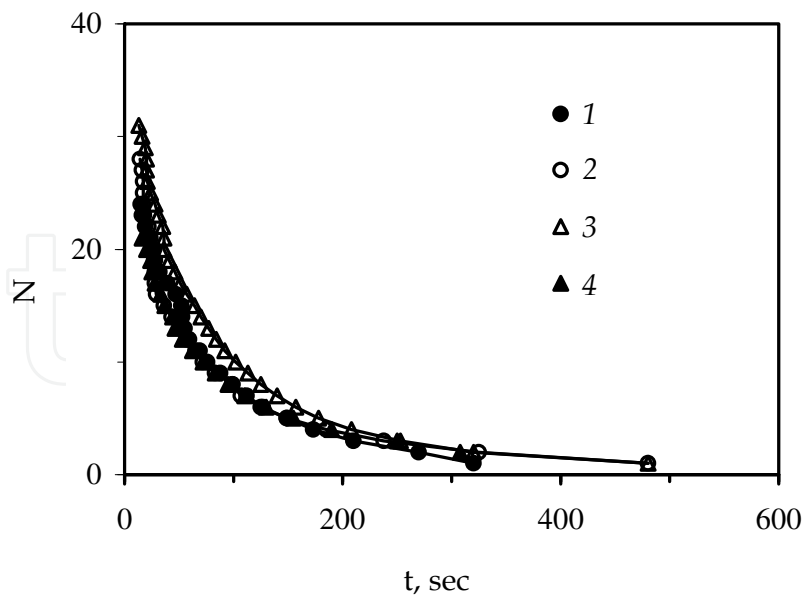


Fig. 4. Time variation of surfactant concentration in center of a drops with diameter of $D_0 = 5.0$ mm at different initial surfactant concentrations: C_d , %: 10 (1); 15 (2); 20 (3)

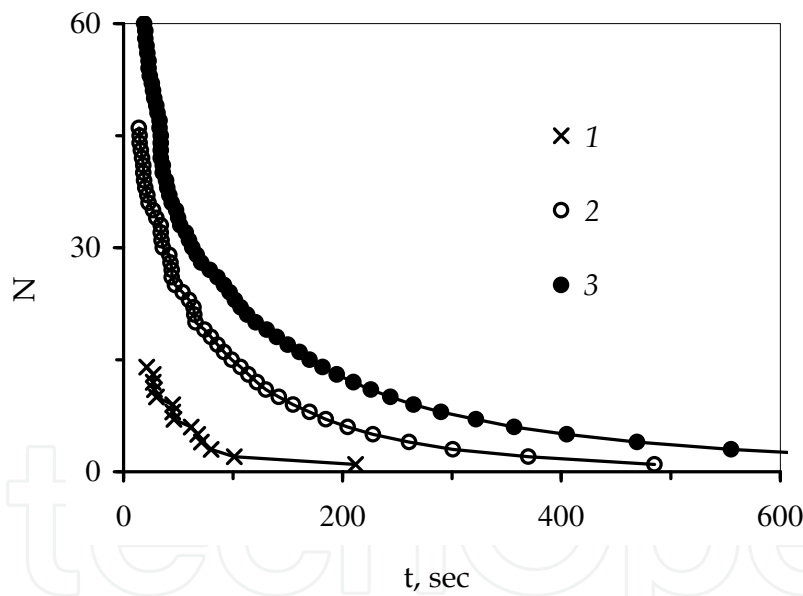


Fig. 5. Time variation of concentration of surfactant for drops at $C_d = 15\%$ with different initial diameters D_0 , mm: 4.2 (1); 6.2 (2); 8.8 (3)

As it is evident from the presented interferograms, the process of surfactant dissolution from the drop proceeds in a quite symmetrical manner, suggesting that at the center of the drop concentration of the surfactant is kept maximal. Fig. 4 shows its variation with time for drops having close diameters but different initial surfactant concentration. It is readily seen that over the selected range of C_d the obtained curves coincide. Since observation of the drop has been made up to the moment of complete surfactant dissolution, such behavior of the curves means that by the time of first measurements, coinciding with the time of cessation of the intensive Marangoni convection (see Fig. 3,c), the content of the surfactant at the center

of the drops with different C_d reaches the same value. From this observation follows the conclusion that a reduction of the difference in the initial surfactant content between different drops (even by two times) occurs at the stage of their formation and development of intensive capillary motion, i.e. during the first 10–12 seconds elapsed after the start of surfactant dissolution.

As we know now, in a horizontal layer, over a rather wide range of C_d variation of surfactant concentration in the drops is described by the same relationship, no matter how many "outbursts" of capillary convection interrupting the gravitational mode of dissolution have occurred. Therefore it is of interest to us to investigate variation of surfactant concentration at the center for drops with different initial diameters (Fig. 5). As might be expected the time of complete withdrawal of the surfactant increases with the size of the drop.

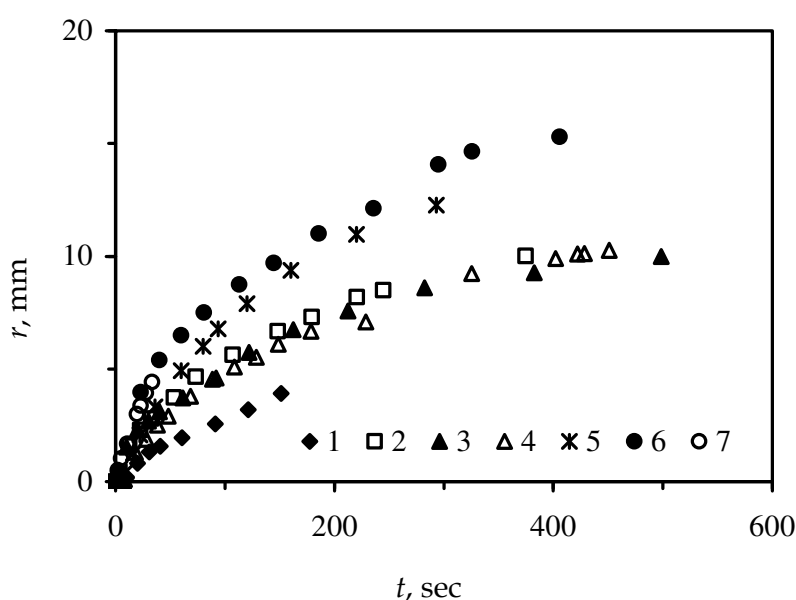


Fig. 6. Time variation of concentration front position for drops with different initial surfactant concentrations: C_0 , %: 1 (1), 3 (2), 5 (3), 10 (4), 15 (5), 20 (6), 30 (7)

The experiments made have revealed also some specific features of the dissolution process for drops with a low content of the surfactant. Among these is the non-linear dependence of the diffusion front velocity on the surfactant concentration (curves 2 and 3 in Fig. 6). It has been found that intensification of the dissolution is caused by the oscillations of the free surface of a quiescent drop, which occurs due to a periodic onset of the local capillary convection at low alcohol concentrations ($C_d \sim 3\text{--}5\%$). Further increase in the initial surfactant concentration results in cessation of the surface oscillations (by this time the Marangoni convection spreads over the whole surface of the drop), which reduces the rate of dissolution (at C_d from 7 to 11%, curve 4). It should be noted that similar periodic ejections of the surfactant from the interface at small values of C_d can be observed in the case of free (spherical) drops of a binary mixture which dissolves in hydroweightlessness conditions (Plateau technique). They occur as weak vertical oscillations of the drop or as periodic up-and-down motions of the emulsion over the drop surface (at $C_d \sim 1\%$) (Kostarev, 2005).

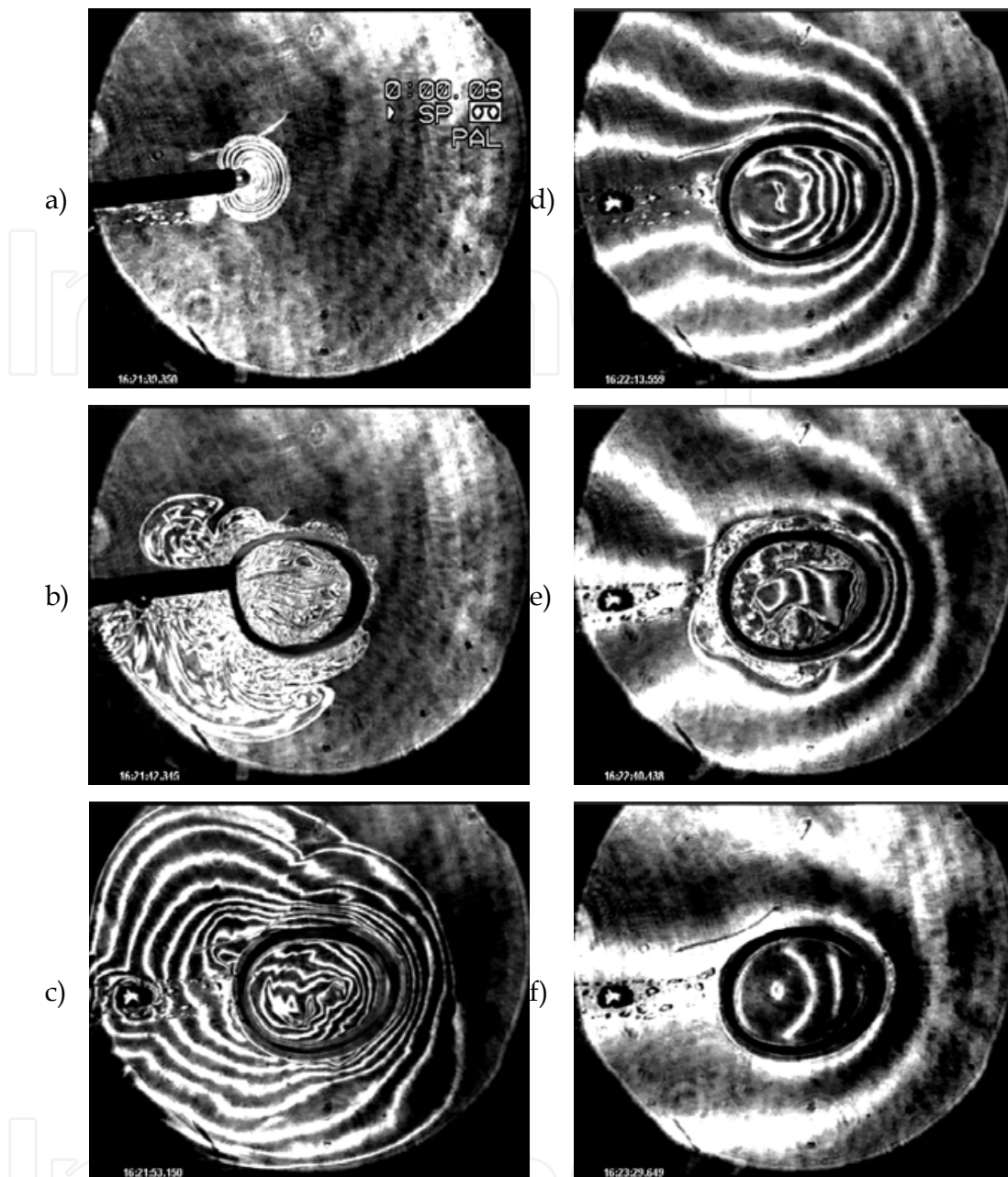


Fig. 7. Distribution of concentration during dissolution of the alcohol from the drop $D_0 = 5.1$ mm with $C_d = 10\%$ in the inclined layer, 1.2mm thick. Angle of inclination $\alpha = 9^\circ$. t , sec: 1 (a), 4 (b), 15 (c), 35 (d), 62 (e), 111 (f)

Since our interest in dissolution of a drop in a thin horizontal layer is primarily dictated by the prospects for simulation of the diffusion processes in liquid systems with non-uniform distribution of surfactants in microgravity, it seems reasonable to give special attention to a change in the structure of the concentration field in a slightly inclined layer. Shown in Fig. 7 are the series of interferograms of the concentration field generated during surfactant dissolution from the drop in the layer inclined at an angle $\alpha = 9^\circ$.

As in the case of a horizontal layer, the diffusion of the surfactant began already in the course of drop formation (Figs. 7,a-7,b) and the alcohol escaping from the drop spread chiefly in the direction of layer rising (Fig. 7,c). The concentration field inside the drop also

underwent rearrangement — the zone of maximum surfactant concentration shifted and ceased to coincide with the geometrical center of the drop (Fig. 7,d). Although the capillary convection is formally independent of the direction and the magnitude of gravitational force, nonetheless the latter has indirect effect on the process. An "outburst" of the Marangoni convection began at the upper part of the drop, accumulating alcohol, which had already permeated through the drop surface but had not left it yet (Fig. 7,e). Thereafter the wave of the capillary motion began to spread downward along the interface. As in the previous case, the process of dissolution ceased in a quasi-diffusion mode, during which the center of the concentration field remained shifted relative the drop center (Fig 7,f).

The tests demonstrated that despite the rearrangement of the concentration field the intensity of mass transfer from the drop does not change with increasing α (at least up to $\alpha \sim 12^\circ$). Evidently this is because the change in the concentration field is nothing but its displacement as a whole with respect to the drop center at a distance proportional to the angle of inclination (Fig. 8). In this case, a decrease in the total flux of the surfactant from the lower part of the drop into the surrounding medium is compensated by an increase of the flux from the upper part.

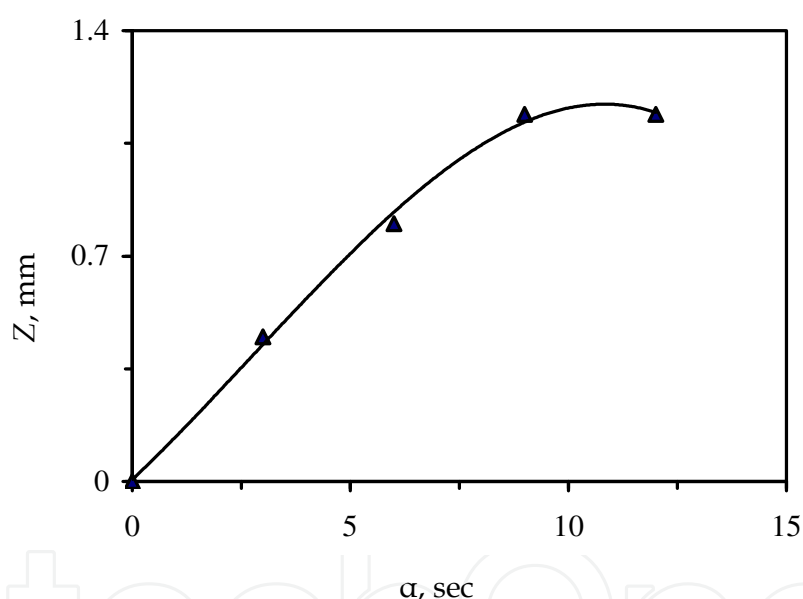


Fig. 8. Displacement of the concentration field center in the drop relative its center during surfactant dissolution in the inclined layer. $D_0 \sim 5.0$ mm; $C_d = 10\%$

4. Surfactant diffusion from drop (space experiment)

4.1 Experimental setup

To obtain the drop in microgravity conditions we used a mixture containing 85% (by mass) of chlorobenzene and 15% of isopropyl alcohol. The distilled water was used as a fluid surrounding the drop. To prevent air bubble formation during long-time storage in microgravity conditions the water and the binary mixture before pouring into the cuvette were degassed by heating them for a long time up to the boiling point. For our experiment we designed and manufactured a small-scale Fizeau interferometer (Fig. 9) (Kostarev *et al.*, 2007).

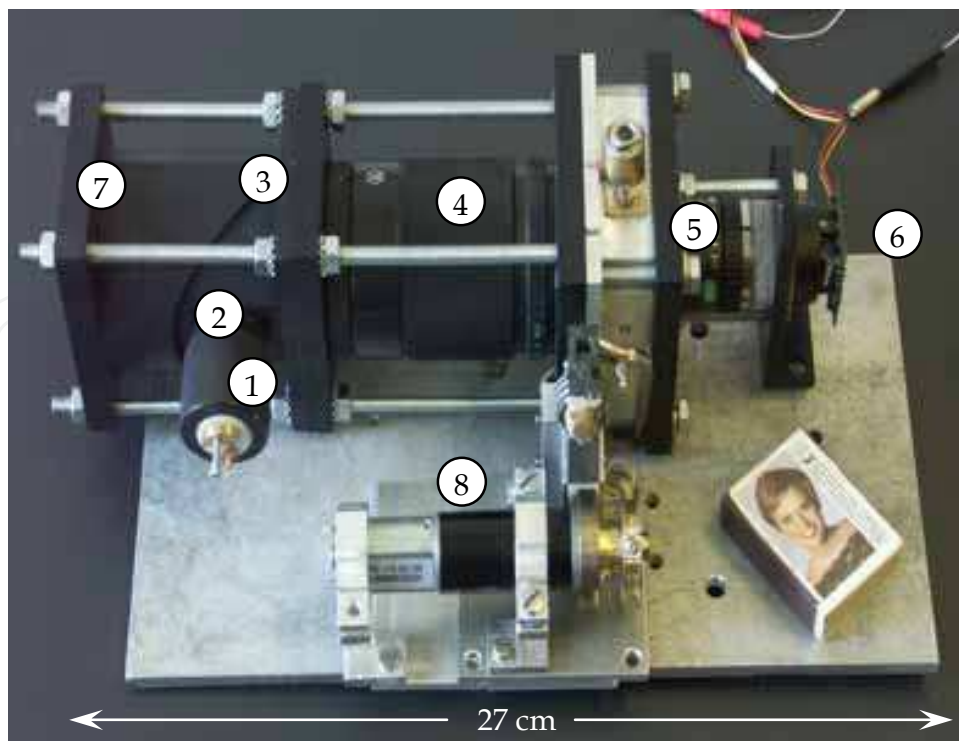


Fig. 9. Scheme of the setup for studying heat/mass transfer processes in microgravity conditions: 1 – laser; 2 – micro-lens; 3 – semi-transparent mirror; 4 – lens-collimator; 5 – Hele-Shaw cell with a drop; 6 and 7 – video cameras, 8 – device for drop formation

The collimator block of the interferometer consisting of microlens 2, semitransparent mirror 3, and lens-collimator 4 generated a plane-parallel coherent light beam of diameter 38 mm, emerging from a semiconductor laser 1. The interferometer was equipped with two analog video cameras 6 and 7, operating respectively with the reflected beam and the beam transmitted through the cuvette 5. Camera 6 registered the interferograms of the temperature and concentration fields in the whole volume of the cuvette and camera 7 was intended to make more detailed records of the process evolution in the central part of the cuvette. The frequency of both cameras was 25 frames a second and the resolving power was 540×720 lines.

For experimental cuvette we chose the Hele-Shaw cell, which was a thin gap 1.2 mm thick between two plane-parallel glass plates 1 with semitransparent mirror coating (Fig. 10). The cell was encased in a metal frame 2 and formed a working cell of the interferometer adjusted to a band of the infinite width. The insert 3 placed in the gap had a hollow, which was used as a cuvette working cavity 35 mm in diameter. The cavity was filled with a base fluid through the opening 4 which was then used to locate a thermal expansion compensator 5. A drop of a binary mixture was formed with the help of a needle of medical syringe which was placed along the cavity diameter. The needle was connected to the binary mixture supply system, which included a bellows for a liquid mixture, multi-step engine with a cam gear, and a device for needle decompression. The backbone of this device is a movable bar connected by means of inextensible thread to a cam mechanism. Prior to experiment the bar was inserted in the needle and the gap between them was sealed. After voltage was applied to the engine the cam began to rotate and first removed the bar from the needle and then bore against the wall of the bellows. As a result, the channel of the needle turned to be open to a flow of the binary mixture from the bellows to the cuvette cavity, where it wetted the

side glass walls and formed a cylindrical drop of prescribed volume at the center of the cuvette. After this the engine was automatically stopped.

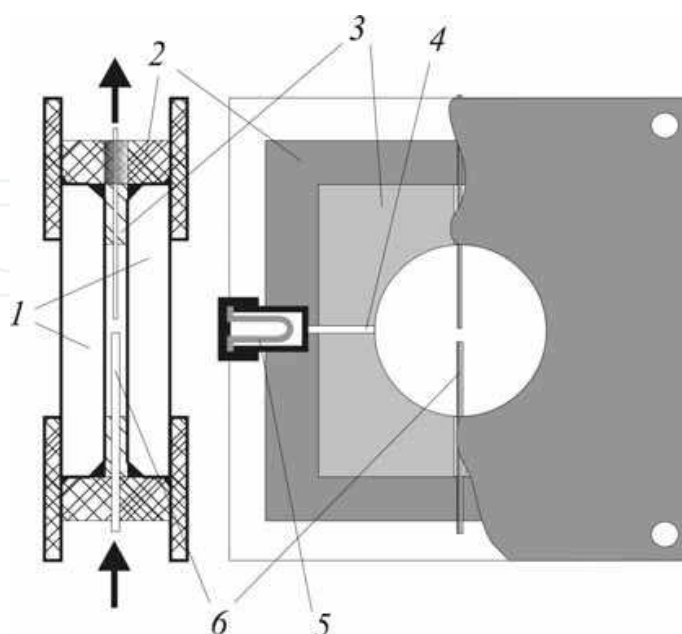


Fig. 10. Scheme of Hele-Shaw cell for studying mass transfer processes:

1 – interferometric glasses, 2 – metal frame, 3 – plastic insert, 4 – opening, 5 – thermal expansion compensator, 6 – tube for drop formation

To determine the flow structure formed during experiment we used the ability of the composed liquid system to form a non-transparent emulsion of water in chlorobenzene and emulsion of chlorobenzene in water while the alcohol diffused through the interface. Focusing the camera 7 (see Fig. 9) on the mid-plane of the cuvette turned the drops of emulsion into analogues of small light – scattering particles which provided flow visualization inside and outside the drop on the background of interferogram of the concentration field.

The total time of the test was 52 minutes. The experiment was carried out at ambient temperature (20 ± 1)°C.

4.2 Results

The analysis of video records showed perfect consistency between the performed experiment and its cyclogram. As the experimental program envisaged during first five minutes records of the interference patterns were made by video camera shooting the central part of the cuvette. The absence of the alcohol distribution near the end of the syringe needle suggested that its hermetic sealing was kept up to the beginning of the experiment. There were no air bubbles on the video records made by the camera, and neither there were the interference bands on the periphery of the images which could be indicative of non-uniform heating of the cuvette.

After switching on the multi-step engine the needle is unsealed so that the binary mixture can be readily supplied to water filling the cuvette. It is to be noted that at first a rather large volume of aqueous solution of the alcohol (up to $6.5 \mu\text{l}$) is ejected from the needle (Fig. 11,a) and only after this the needle forms a drop of a binary mixture with a clear-cut interphase

boundary (Fig. 11,*b*). The maximal concentration of the alcohol in this drop is about 5.5%. The reason for appearance of the aqueous solution of the alcohol in the needle is penetration of water from the cavity into the channel of the needle after removal of the sealing bar.

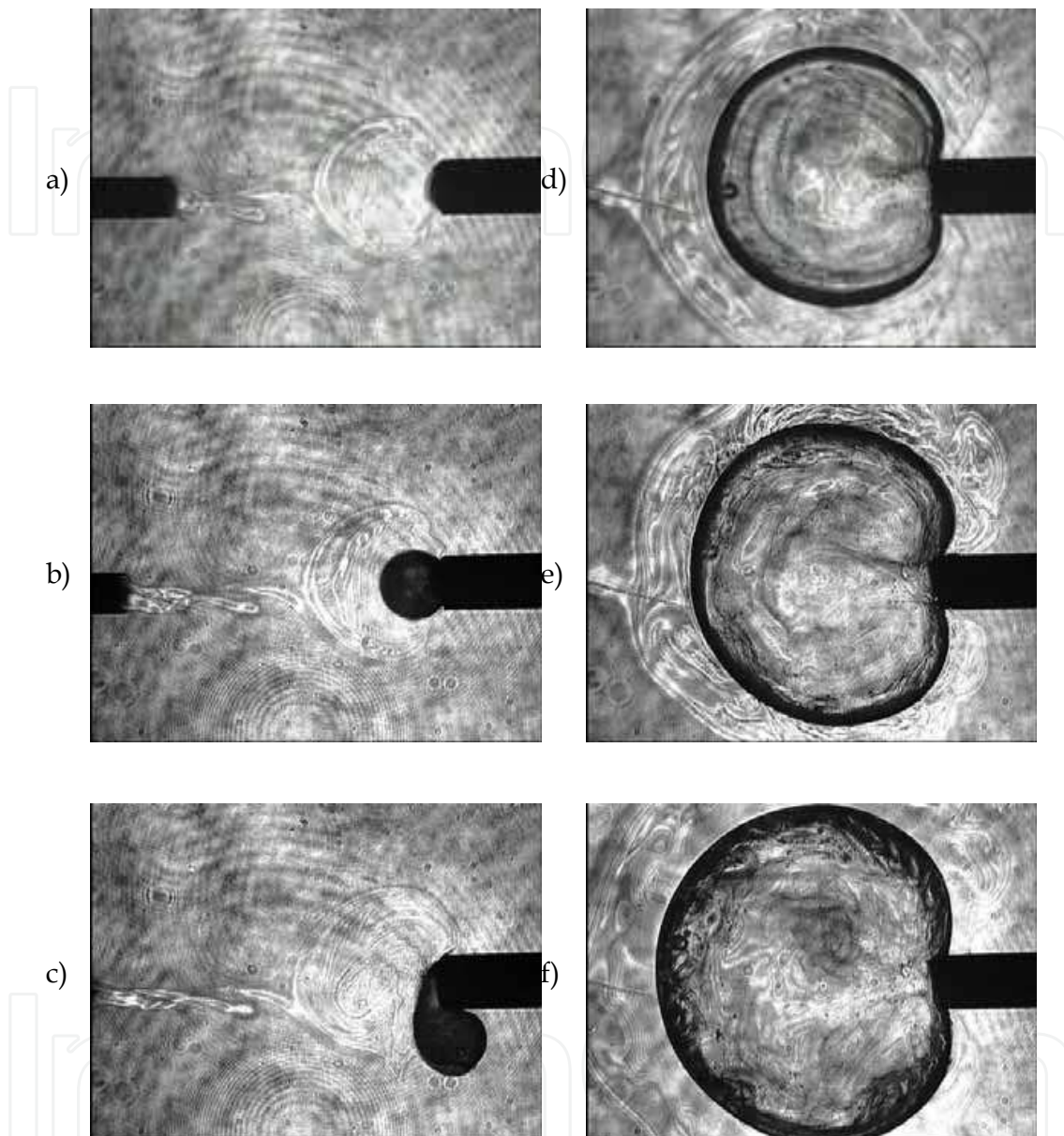


Fig. 11. Evolution of the concentration field and flow structure during the drop formation. External diameter of needle is 1.0 mm. Time from the test outset t , sec: 4.5 (*a*), 4.9 (*b*), 5.1 (*c*), 8.2 (*d*), 8.6 (*e*), 10.2 (*f*)

Since ejection of the drop is preceded by appearance of the alcohol solution the drop during first seconds of its existence is in a quiescent state being surrounded by a similar media. Then as the drop grows it comes into contact with pure water which leads to initiation of intensive solutocapillary motion of the drop surface due to generation of the surface tension difference. As a result, the drop executes several oscillatory motions with large amplitude (Fig. 11,*c*) like a drop in the known Lewis and Pratt experiment (Lewis & Pratt, 1953). The oscillations of the drop extend the boundaries of the region containing liquid enriched with

the alcohol. This leads to a decrease of the concentration gradient at the interface and the growing drop again quiets down. Approximately at the same time the drop reaches the lateral boundaries of the cavity gradually changing its shape from a spherical to a cylindrical. As the drop turns into a cylindrical drop its internal structure becomes more and more observable.

Further increase of the drop size is accompanied by formation of several internal solutal zones in the vicinity of its boundary. In these zones transfer of the surfactant occurs with quasi-diffusional velocities (the flow of the mixture caused by injection of the solution into the drop is concentrated in its central part, Fig. 11,*d*). A jump-wise increase of the feeding velocity by 2 times (at $t = 8.3$ sec) causes an abrupt intensification of the motion inside the drop, which breaks down the established concentration field. Again the vortex flow spreads over the whole drop while pure water reaches the surface of the drop in the zone of its contact with needle. This leads to a repeated outburst of capillary convection (Fig. 11,*e*) Development of the Marangoni convection is accompanied by deformation of the drop itself and the surrounding front of surfactant concentration, which gains a quasi-periodic structure. Then, as in the first case, a flow of the diffused surfactant into the zone, where pure water comes into contact with the solution of the drop, causes retardation of the capillary motion, which coincides in time with cessation of mixture supply to the drop (Fig. 11,*f*). At this moment the maximal diameter d_0 of drop reaches 6.2 mm.

When the forced motion in the drop ceases, the water emulsion, captured during surfactant diffusion at the time of intensive convection and kept near the drop surface, begins to penetrate deep into the drop. The penetrating emulsion forms a clearly delineated layer (Fig. 12,*a*). In the gap between this layer and the drop surface one can watch the formation of a light layer of the mixture, which has lost most of the surfactant due to diffusion (a decrease in the surfactant concentration leads to an abrupt change in the index of light refraction, Fig. 12,*b*). Propagation of emulsion with velocities of about 0.2 mm/sec is supported by a slow large-scale motion of the mixture in the drop caused by capillary eddies formed near the needle (Fig. 12,*c*).

The source of eddy formation is the alcohol, which diffuses from the needle after cessation of mixture supply. It creates a surfactant concentration difference at the free surfaces of the air bubbles, generated near the needle due to a decrease of air solubility in the fluid of the drop, in which alcohol concentration decreases. Most of the bubbles are formed at the drop boundary and then migrate deeper and deeper into the drop under the action of capillary forces. The average diameter of the bubble is of order 0.1 mm, and the maximum diameter is ~ 0.3 mm. Apart from the eddy flow there is a slow capillary motion of the mixture over the drop surface toward its far pole (opposite to the tip of the needle). This flow also contributes to the emulsion motion.

The motion of emulsion is accompanied by coalescence of part of its droplets, which settle down on the walls of the cavity. (The arising droplets can be seen due to a trace of emulsion kept in the stagnation zone behind them, Fig. 12,*d*). As the emulsion layer moves away from the boundary, one can observe development of a small-cell motion near the bubbles, which are in the diffusion gradient of the surfactant at the drop boundary. What is interesting, detachment of these bubbles from the drop interface as well as the local displacement of the drop boundary due to reduction of its area during diffusion of the surfactant causes a specific stochastic fluttering of the drop surface.

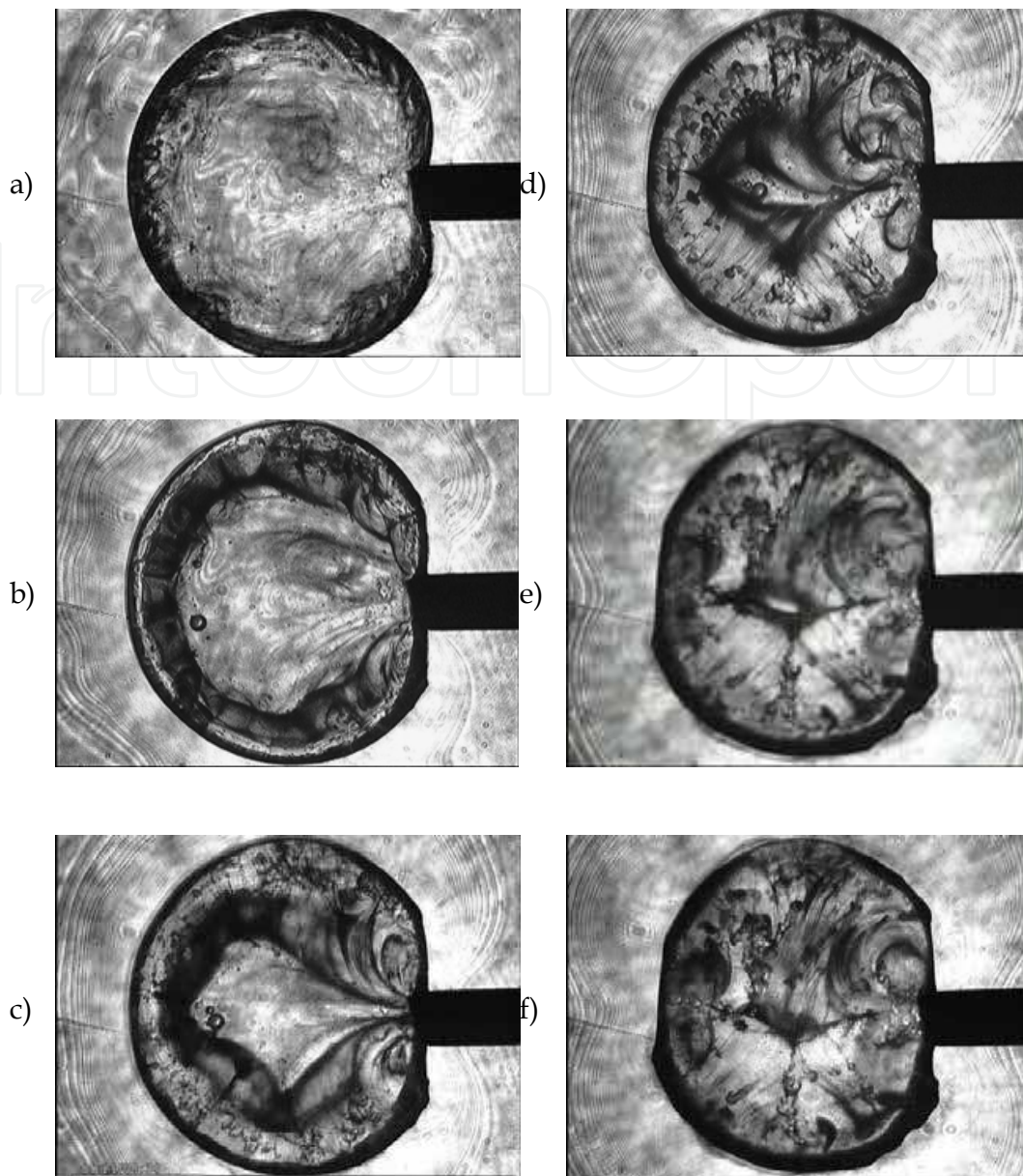


Fig. 12. Evolution of the concentration field and flow structure during surfactant dissolution process. Time from the test outset t , sec: 15.5 (a), 38.7 (b), 88.4 (c), 163 (d), 251 (e), 273 (f)

The cell motion reaches maximum intensity at the drop pole opposite to the tip of the needle (evidently due to the absence of flows generated earlier in this region). The air bubbles formed in the immediate neighborhood, accelerates the motion of mixture from the center of the drop and also favors the development of the cell motion. The arising flow is of three-dimensional pattern and as the times goes it occupies an increasingly growing space and even deforms the solutal front, which moves away from the drop (Fig. 12,e). Simultaneously there occurs another interesting phenomenon – settling of gas bubbles at the cavity walls. During sedimentation the bubbles take the form of irregular semi-spheres. This effect can be observed at the time when the bubbles are in the emulsion cloud.

After five minutes from the beginning of drop formation the velocity of the fluid flow in the drop decreases practically to zero (Fig. 12,f) and the volume of the drop reduces to 0.9 of its maximum (Fig. 13).

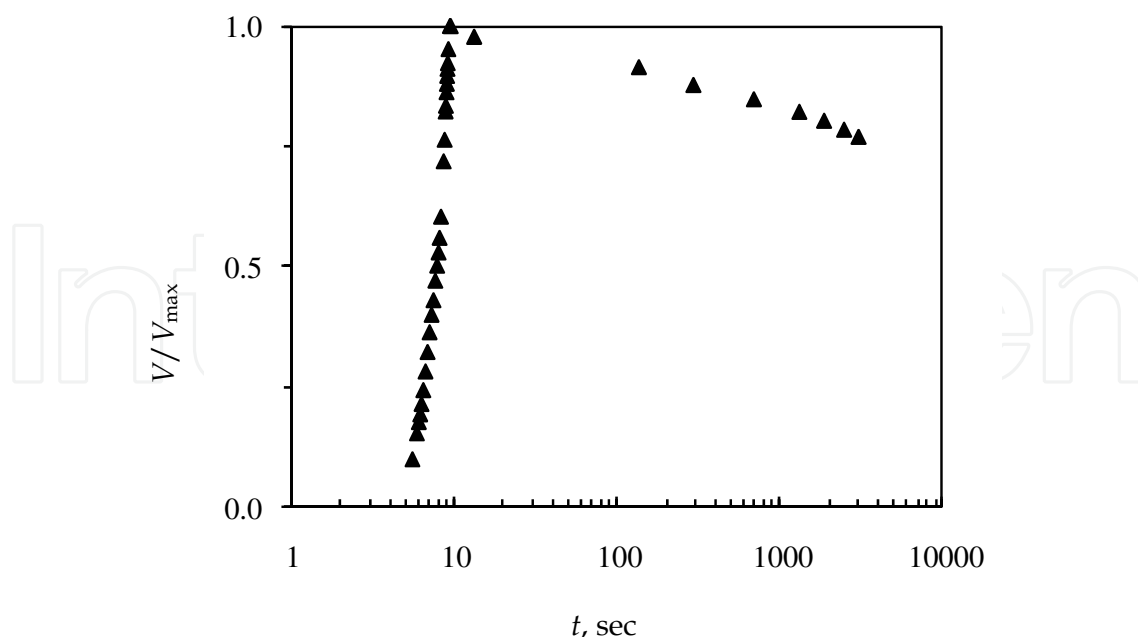


Fig. 13. Variation of the relative volume of dissolving drop with time

Fig. 14 shows a series of interferograms of the concentration field in the vicinity and inside the drop at different moments of time. As it is seen from the figure, in the following, after first five minutes, the only observable events are gradual dissolution of the emulsion and variation of the surfactant concentration gradient in the radial direction. Apart from this a decrease of the alcohol concentration in the region near the drop boundary leads to a growth of the surface tension and, as a result, to local jump-wise displacement of the drop boundary while the area of the latter decreases.

Hence, based on the analysis of the obtained video records we can draw a conclusion that during diffusion of the surfactant from the drop at least three times there were favorable conditions for the development of the intensive Marangoni convection. However, all the observed capillary flows rapidly decayed. In the first two cases – during drop formation and a change in the mixture feeding regime – the Marangoni convection decay was provoked by a flow of a surrounding fluid with higher surfactant concentration into the zone of the capillary motion, which eliminates the concentration difference along the interface. On the other hand, generation of such surfactant distribution in the vicinity of the drop was made possible only in the absence of the Archimedean force with the result that molecular diffusion became a governing factor in the process of mass transfer outside the drop. In the third case, when the Marangoni convection was initiated near the gas bubbles inside the drop, the reason of its decay was a decrease of surfactant percentage in the mixture filling the needle channel and rapid recovery of the surfactant distribution homogeneity in the region near the bubbles due to convective mixing.

Video recording of the central part of the cuvette has made it possible to trace the evolution of initiated flows, whereas records of the general view of the drop (Fig. 15,a) allow us to investigate propagation of the concentration front from the dissolving drop of the binary mixture and to establish the relationship between the position of its boundary and time (Fig. 15,b). It is readily seen that propagation of the concentration front is described fairly

well by the power law with the exponent $1/3$. Over the whole period of the experiment position of the concentration front changed by 5 mm suggesting that propagation of the surfactant occurred with diffusion velocities. According to measurements made in the second half of the experiment, the concentration field has no preferential direction of propagation, which allows us to suppose that the value of the residual accelerations on the satellite "Foton-M 3" during the experiment was no higher than $10^{-4} g_0$.

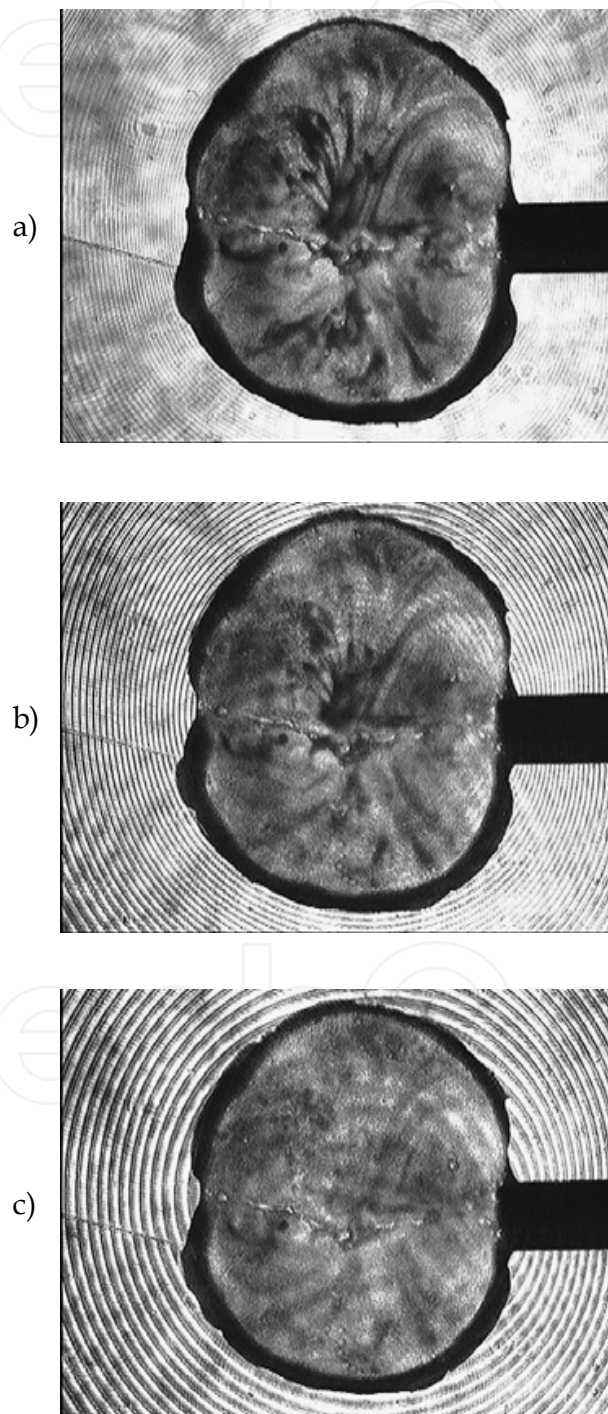


Fig. 14. Evolution of the concentration field and flow structure during surfactant dissolution process. Time from the test outset t , min: 15.2 (a), 19.3 (b), 28.8 (c)

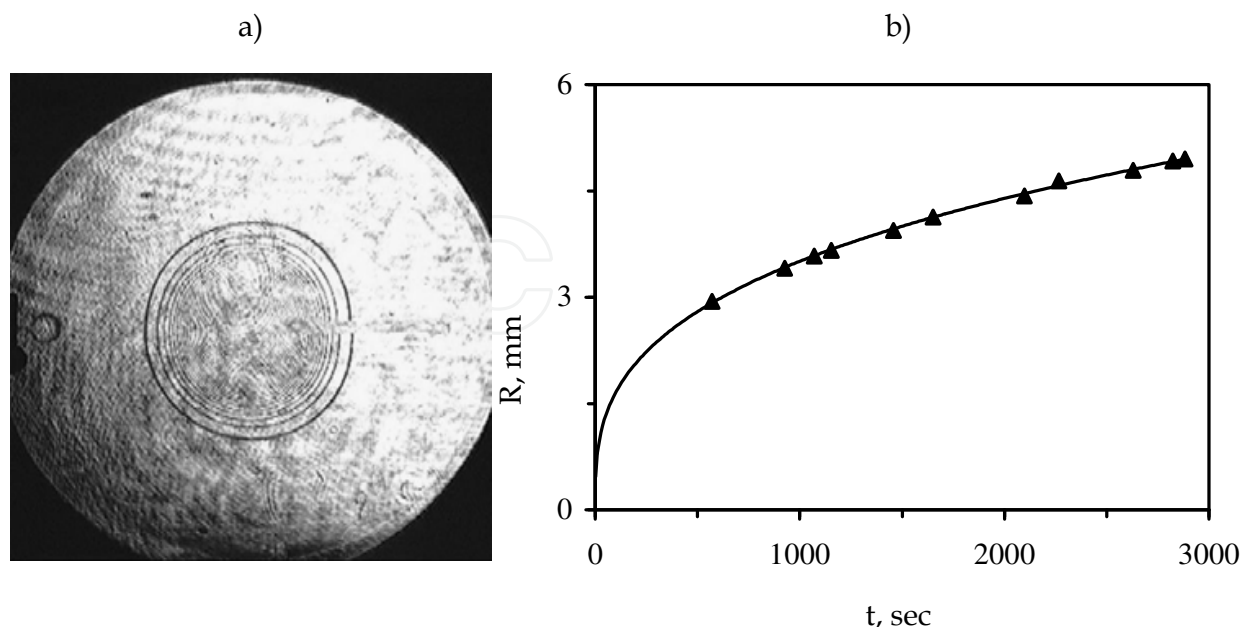


Fig. 15. View of distribution of surfactant concentration around drop (a) and variation of the boundary position (b) of concentration field with time

A detailed structure of the concentration field generated by surfactant diffusion (Fig. 16) was defined by making use of the computer-aided overlapping of images obtained from both video cameras (such an approach was used to solve the problem with relatively low value of their resolving power). Since only one video recorder was used for recording, we chose for overlapping the images shot by different camera with the shortest time span between them. It should be emphasized that distribution of the surfactant concentration outside the drop was obtained by way of direct measurements, which were made based on the interferograms starting from the field (front) boundary. It was impossible to apply this approach inside the drop because of the unknown value of the surfactant concentration at the drop boundary. This value remained unknown due its jump-wise change provoked by a difference in the chemical potentials. We determined it from the curves, which were plotted based on the coefficient of the equilibrium distribution of the isopropyl alcohol in the chlorobenze-water system under the assumption that the dissolution process was quasi-equilibrium due to predominance of diffusion. For the selected system of fluids the value of this coefficient was 0.12 in 15% water solution of the alcohol and as the alcohol concentration decreased, this coefficient also decreased to 0.10.

As it follows from Fig. 17, alcohol concentration at the drop surface at the time when the motion of the mixture in the drop ceases, is $\sim 14\%$, which actually coincides with the initial concentration of the alcohol in the binary mixture of the drop. Note that at the end of the test the surfactant concentration at the drop boundary decreased approximately by two times. This reduction can be approximated with the least error by the exponential relationship. For the sake of comparison, on the Earth under conditions of maximum suppression of the gravitational convection the drop of the same volume completely lost the alcohol in a matter of ten minutes.

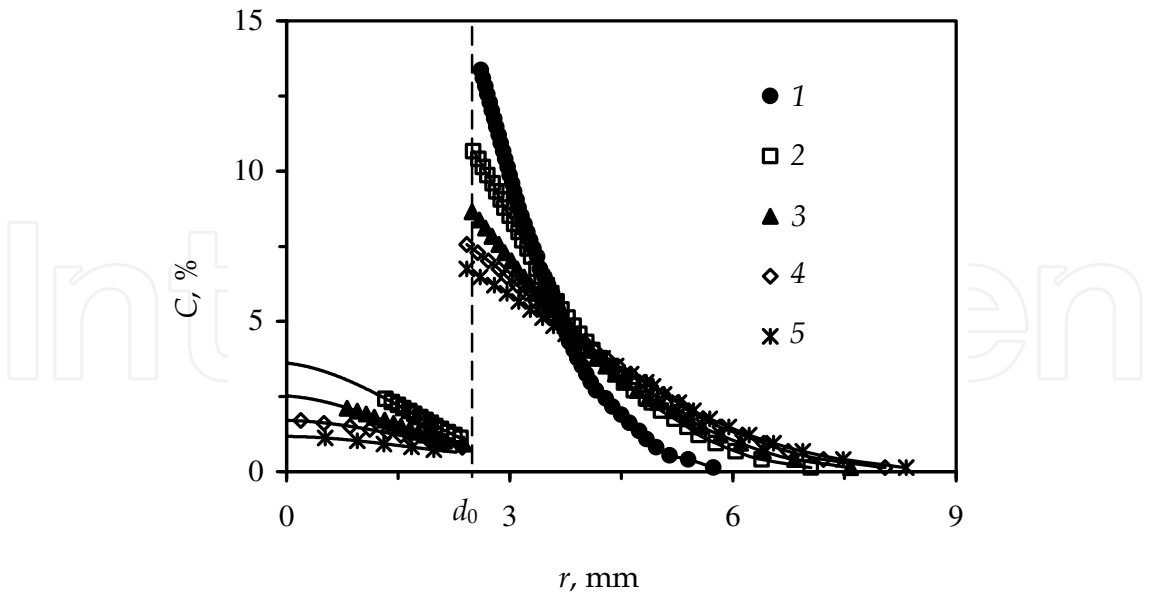


Fig. 16. Radial distributions of surfactant concentration in the vicinity and inside the drop at various time moments. t , min: 4.9 (1), 21.3 (2), 31.0 (3), 42.5 (4), 50.7 (5)

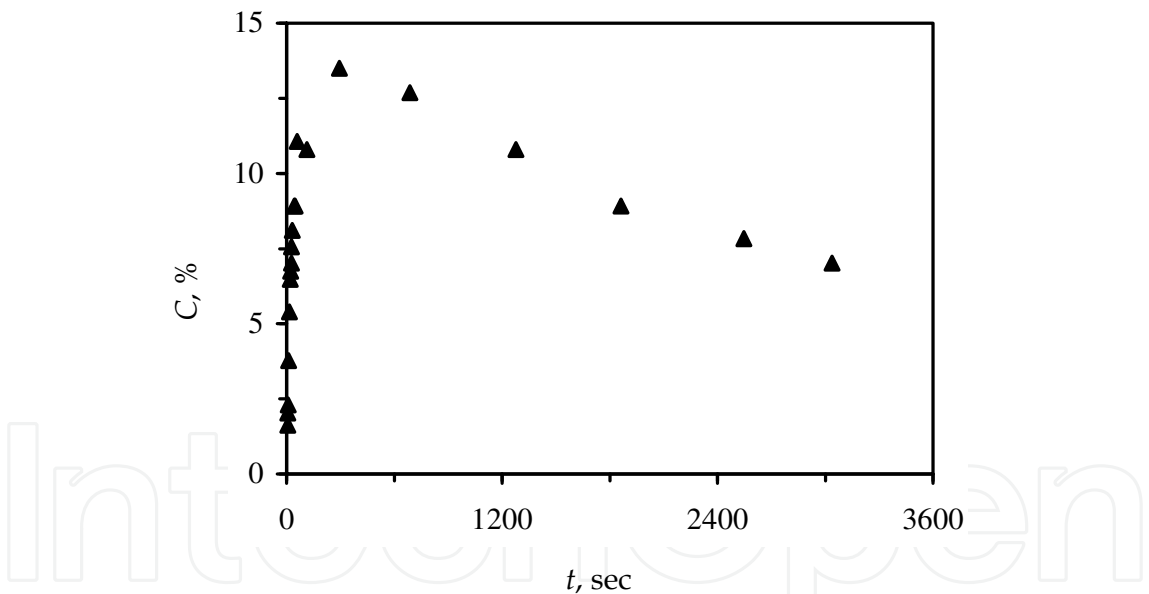


Fig. 17. Variation of surfactant concentration in water near the drop surface with time

5. Drop saturation by surfactant from homogeneous solution

In this series of test the initial mass concentration C_0 of the alcohol in the solution ranged from 1% to 50%. Fig. 18 shows two series of the interferograms reflecting the evolution of the alcohol distribution in the drop at different initial concentrations of alcohol in the solution. It is seen that at $C_0 \leq 10\%$ absorption of alcohol occurs without the development of the capillary convection in spite of the interference of the gravity force, which generates the vertical concentration gradient and, accordingly, the gradient of the surface tension. The

latter seemed to be not large enough to produce shear stresses capable of deforming the adsorbed layer, which was formed at the interface from the impurities found in water (Birikh *et al.*, 2009). In the absence of the Marangoni convection, alcohol was slowly accumulated at the upper part of the drop. As soon as an increasingly growing thickness of the alcohol layer caused an additional optical beam path difference of half of the light wave length, the color of the drop on the interferogram changed (Figs. 18,*b-18,c*).

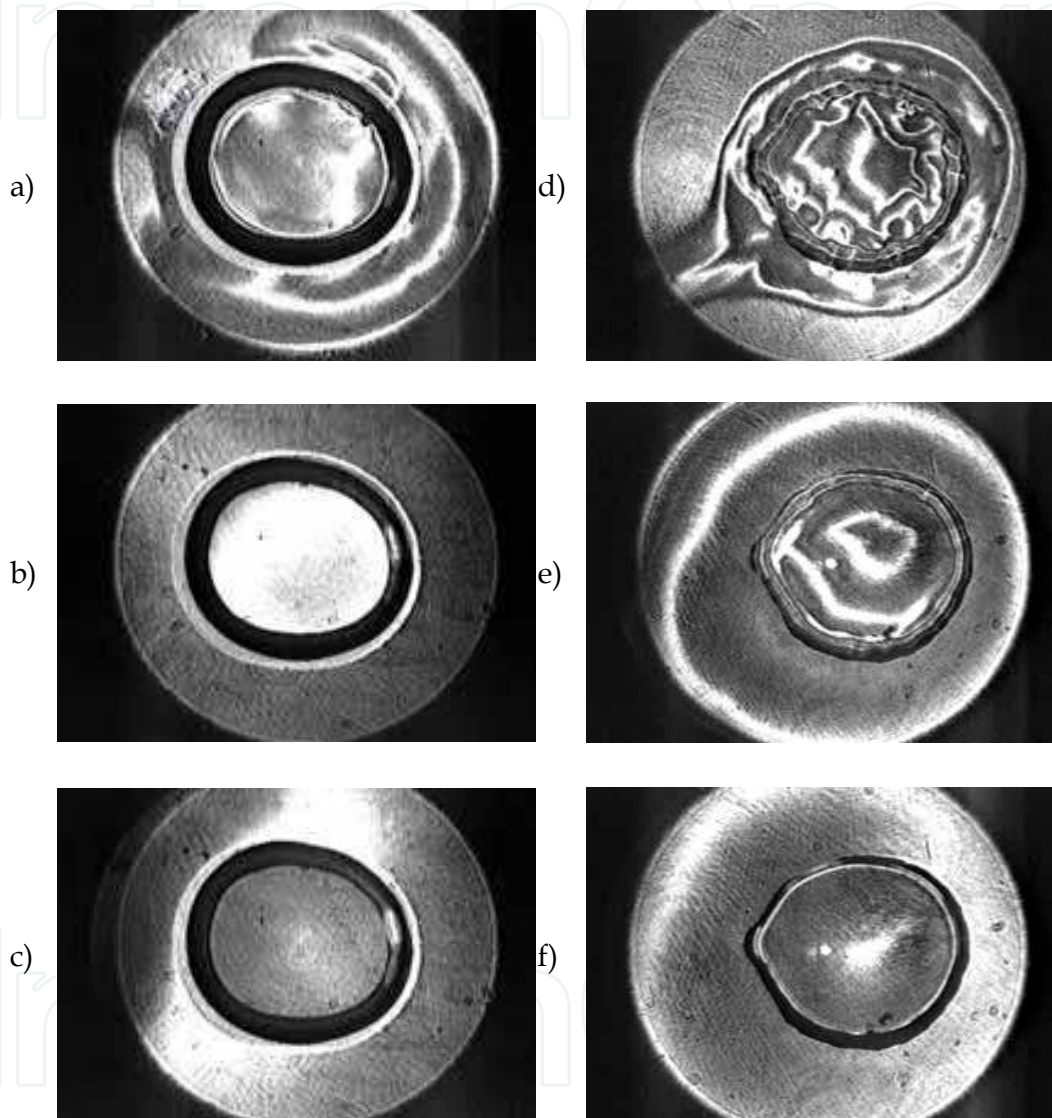


Fig. 18. Saturation of the chlorobenzene drop with isopropyl alcohol from its solution filling a horizontal Hele-Shaw cell. $C_0 = 10\%$, $D_0 = 5.2$ mm; t , min: 0.5 (*a*), 7.0 (*b*), 10.0 (*c*); $C_0 = 20\%$, $D_0 = 5.4$ mm; t , min: 0.1 (*d*), 1.0 (*e*), 6.0 (*f*)

At $C_0 \sim 20\%$ the gradients of surfactant concentration become higher than the threshold values which results in the development of a fine-cell capillary motion at the drop surface. With the growth of surfactant concentration the velocity of the surfactant flow into the drop increases and the gravitational force has not managed to smooth the layer of alcohol along the drop diameter. Due to the fact that the layer is formed from alcohol, rising along the lateral surface of the drop, its thickness is found to be larger at the layer edges. On the

interferograms the radial variation in the layer thickness is represented by a system of concentric isolines, which merge with the passage of time at the center of the drop (Figs. 18,*d* -18,*e*). On the drop periphery one can readily see a thin layer of rising alcohol, which has diffused through the interface (Fig. 18,*f*).

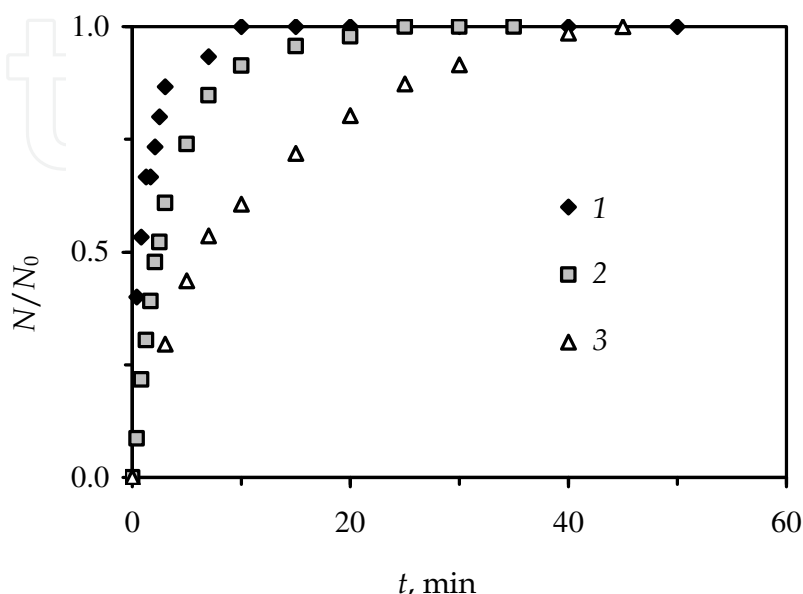


Fig. 19. The relative number of isolines inside the drop as a function of time for different concentrations of solution C_0 , %: 10 (1), 20 (2), 30 (3). The initial drop area $S_0 \sim 35 \text{ mm}^2$

In Fig. 19, a relative number of the interference bands vanishing at the center of the drop is plotted versus the time elapsed from the moment of drop formation for solutions of different concentrations (for normalization we used the maximum number of the bands obtained in each cases). The analysis of the curve behavior shows that duration of the phase, in which a convective mass transfer dominates over a pure diffusion transfer, rapidly increases with the growth of surfactant concentration in the solution.

Absorption of alcohol from its solution should cause a growth of the drop volume, which in the case of the cylindrical drop with the fixed thickness is manifested as an increase of its area. Indeed, saturation of the drop with alcohol was accompanied by a change of its area. However, this variation was of a complicated nature, which was specified by the initial concentration of the surfactant in the solution (Fig. 20). Such a behavior of the absorbing drop can be explained by an increase in the reciprocal solubility of water and chlorobenzene with a growth of concentration of their common solvent, viz., the content of alcohol in their solutions. The maximum increase ($\sim 20\%$) in the drop area was observed at the initial stage of its saturation at $C_0 = 40\%$ (curve 3 in Fig. 20). Then the drop began to dissolve due to increasing diffusion of chlorobenzene in the surrounding solution. A delay in dissolution was caused by the insufficient content of the surfactant inside the drop. The desired concentration was achieved only some time after injection of the drop into the solution. In the solution containing 45% of alcohol (curve 4 in Fig. 20) concentration of the absorbed surfactant at the drop boundary immediately reached the value, at which chlorobenzene began to dissolve in the surrounding solution. The process of the surfactant extraction turned into the reverse – dissolution of the extragent.

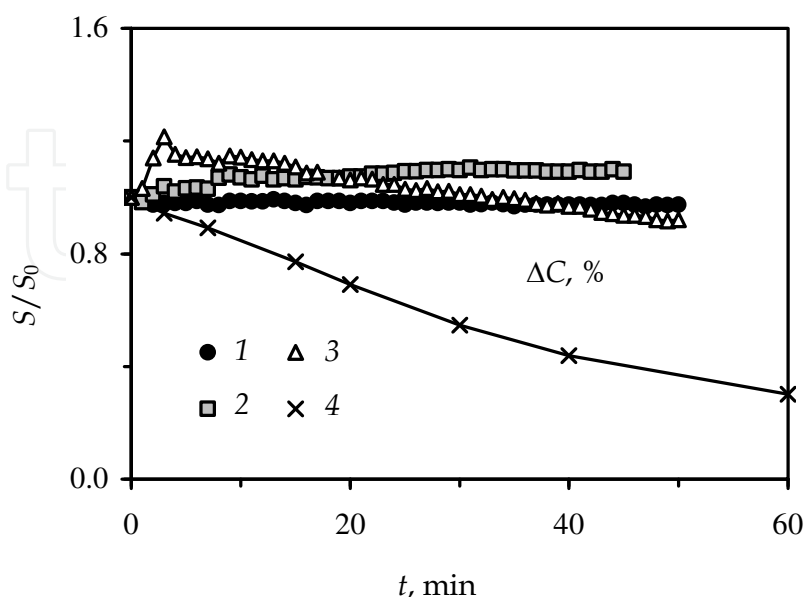


Fig. 20. The relative area of the chlorobenzene drop as a function of time for isopropyl solutions of various concentrations. The initial drop area $S_0 \sim 35 \text{ mm}^2$. C_0 , %: 10 (1), 30 (2), 40 (3), 45 (4)

Dissolution of chlorobenzene gave rise to an intensive gravitational flow in the surrounding solution. This process every so often was accompanied by generation of both the vertical and longitudinal (lying in the layer plane) difference of the surfactant concentration at the drop surface provoking the development of a large-scale capillary flow.

In our case, such a flow occurred in the form of two quasi-stationary vortices lying in the horizontal plane (Fig. 21). Note that the flow was sustained by a small difference ($\sim 3\%$) in the surfactant concentration between the "western" and "eastern" poles of the drop. The initial solution entrained by the flow reached the drop surface in the form of the concentration "tongue", which then split into the streams flowing round the drop. As they spread along the drop surface they lost part of alcohol due to its diffusion. After that they again merged into a single flux, which drifted away from the drop carrying part of alcohol-chlorobenzene mixture.

In turn, alcohol penetrated into the drop and formed two fluxes, which first moved along the interface and then after collision at the western pole of the drop spread deep into the drop generating a two-vortex flow. The flows initiated inside and near the drop closely resemble in structure the convective flow near the drop absorbing the surfactant from its stratified solution in the vertical Hele-Shaw cell (Kostarev *et al.*, 2007). However, under conditions of maximum suppression of gravitational convection the considered flow remains quasi-stationary – in contrast to the flow in a vertical cell, which at the similar surfactant concentration differences is of the pronounced oscillatory nature. At $C_0 = 50\%$ the phase boundary between the drop and the solution disappears leading to the formation of a three-component liquid mixture. Phase separation of the fluid system vanishes within the first two minutes after placing the drop into the surfactant solution.

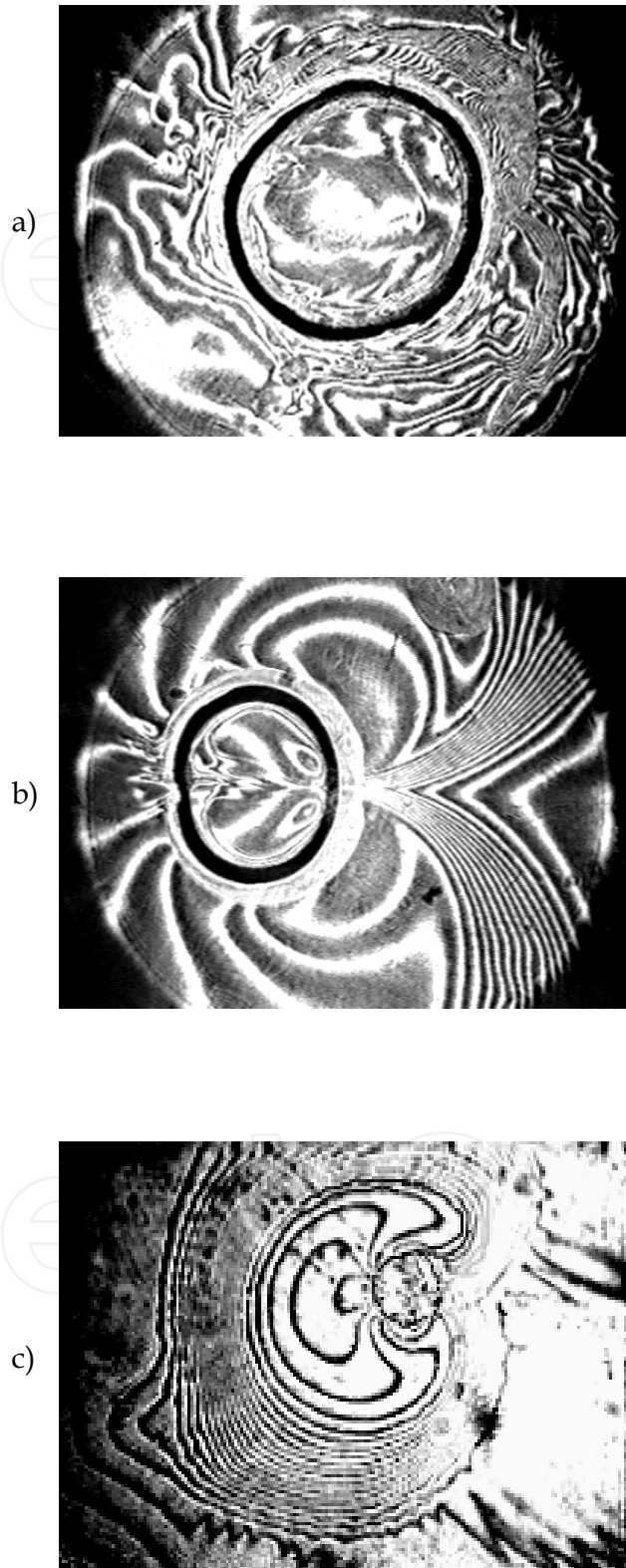


Fig. 21. Distribution of concentration of isopropyl alcohol during its absorption by the drop of chlorobenzene from the solution with initial concentration $C_0 = 45\%$. $D_0 = 6.5$ mm. t , min: 0 (*a*); 40 (*b*); 190 (*c*, general view of the cell flow with the drop in center)

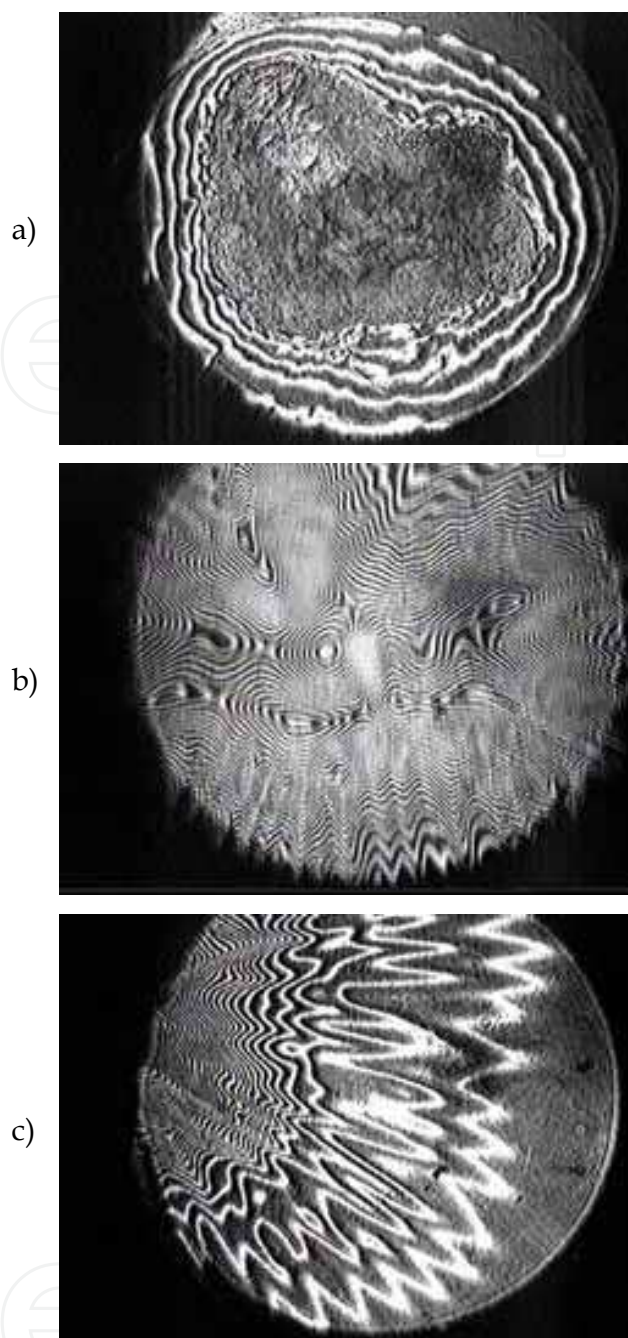


Fig. 22. Dissolution of a drop of chlorobenzene in 50% solution of alcohol. t , min: 1.25 (a); 9.0 (b); 11.2 (c)

Fig. 22 illustrates the main stages of drop dissolution in the surrounding solution at $C_0 = 50\%$. Absorption of alcohol at the moment of drop formation diminishes the interface surface tension to an extent that it turns to be impossible to form a cylindrical drop even in one-millimeter clearance. Nevertheless, the original drop has an interface with sufficient curvature, owing to which the probing light beam scatters. As a result the drop interface is seen on the interferogram as a grey spot (Fig. 22,a). Then the drop surface increases because the drop spreads out over the cavity bottom as the surface tension continuously decreases. Further dissolution is accompanied by deformation of both the drop interface and the boundary between the drop and a solid substrate. Disappearance of the interface in the fluid

system makes the mixture optically transparent because the jumps of the refraction coefficient have vanished. Fig. 22,*b* presents the interferogram of the optical inhomogeneity caused by inhomogeneous concentration of chlorobenzene at the place of the former drop. It is seen that a transition zone between the solution and the mixture with higher content of chlorobenzene has a well-defined relief, which is similar to the relief of the free surface of the drop. In Fig. 22,*c* we can see part of the concentration inhomogeneity picture with typical distribution of chlorobenzene in alcohol in the form of "fingers", whose origination can be attributed to a flow of chlorobenzene down the spatial inhomogeneities of the transition zone.

The period of spatial perturbations of the drop-solution interface, repeated further by the relief of the transition zone of the concentration inhomogeneity, is defined by the physico-chemical properties of the interacting fluids. As for the solution, these properties are strongly dependent on surfactant concentration. Indeed, according to the results of measurement the angular distance between the "fingers" increases with a growth of the surfactant solution concentration (Fig. 23).

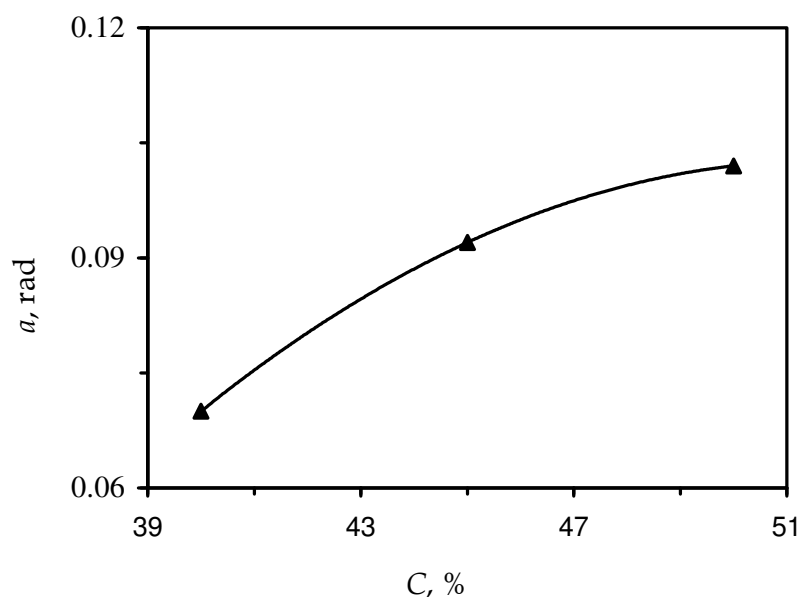


Fig. 23. Variation of the angle between "fingers" with the growth of initial concentration of the surfactant solution

6. Conclusion

As seen from a comparison of space and terrestrial experiments, the data obtained in microgravity differ markedly from the results of the laboratory study of surfactant diffusion in a thin horizontal layer. In the later case a small coefficient of surfactant diffusion facilitated generation of the density difference in the originally homogeneous surrounding fluid. This difference was large enough for development of the gravitational motion inside and outside the drop. Nevertheless a relative contribution of the Marangoni convection to the process considerably increased — the action of the capillary forces mainly determined the rate of mass transfer at the beginning of surfactant diffusion. Only a decrease in the surfactant concentration below some critical value led to regeneration of the gravitational-diffusion mechanism of mass transfer, yet its action was repeatedly interrupted by the

"outbursts" of intensive capillary convection. Because of a three-dimensional structure of the flows in the laboratory conditions, the application of the interference method posed many difficulties; only the qualitative characteristics were used for description of the evolution of concentration fields. However, the laboratory experiments allowed us to make an optimal choice of the parameters for the space experiment and to prepare its preliminary cyclogram. The space experiment "Diffusion of the surfactant from a drop" was successful. The sensitivity of the new setup proved to be an order of magnitude higher than that of the shadow device "Pion-M" used on the "Mir" space station. The weight of the setup was reduced by more than an order of magnitude, and its external dimensions were also downsized. The interferometer can operate in the automatic regime allowing performance of experiments onboard the unmanned space vehicles. The obtained data supported the view that in microgravity conditions the mass transfer processes involving surfactant diffusion through the interface can proceed without excitation of intensive capillary convection.

Because of diffusion in the absence of capillary convection, the surfactant concentration reaches rather high values at both sides of the drop surface. This leads to much greater extent of mutual dissolution of the base fluids compared to the terrestrial conditions. Therefore, the interface failure in such a system can occur at much lower concentration of the surfactant which plays the role of a common solvent for both the base fluids. On the one hand, this allowed a more exact computation of the value of this concentration, which is an essential prerequisite for development of the theoretical grounds of phase transitions in three-component liquid systems. On the other hand, reduction of the limiting concentration opens the way to intensive experimental studies of the hydrodynamic effects involving the interface failure.

At the same time, based on terrestrial simulation data, we can expect the development of a large-scale Marangoni flow around the drop absorbing the surfactant from the homogeneous surfactant solution in microgravity conditions. Such a different evolution of mass transfer processes in the surfactant solution emphasizes again the importance of experimental investigations in real microgravity conditions.

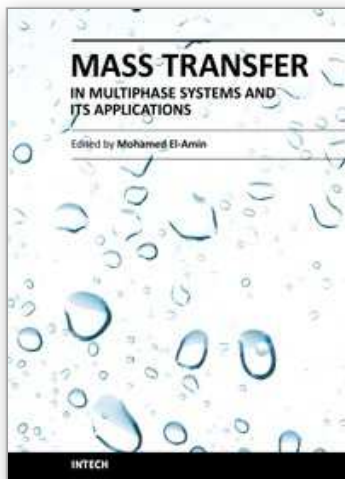
7. Acknowledgements

The work was supported by Russian Foundation of Fundamental Research under project No 09-01-00484, joint project of SB, UB and F-EB of RAS (116/09-C-1-1005) and the program of the Department of Power Engineering, Mechanical Engineering, Mechanics and Control Processes of RAS No 09-T-1-1005.

8. References

- Agble, D. & Mendes-Tatsis, M.A. (2000). The effect of surfactant on interfacial mass transfer in binary liquid-liquid systems. *J. Heat and Mass Transfer*, Vol. 43, p. 1025.
- Amar, A.; Groß-Hardt, E.; Khrapitchev, A.A.; Stapf, S.; Pfennig, A. & Blümich, B. (2005). Visualizing flow vortices inside a single levitated drop. *J. of Magnetic Resonance*, Vol. 177, No. 1, pp. 74–85.
- Bratukhin, Yu.K.; Kosvintsev, S.R. & Makarov, S.O. (2001). Droplet motion induced by diffusion of soluble surfactant to the external medium: theory. *Colloid J.*, Vol. 63, No. 3, pp. 326–332.

- Burghoff, S. & Kenig, E.Y. (2006). A CFD model for mass transfer and interfacial phenomena on single droplets. *AIChE J.*, Vol. 52, No. 12, pp. 4071–4078.
- Gustafson, S.E.; Kjellander, R.A.E. & Rolf, A.E. (1968). An interferometer for direct recording of refractive index distributions. *Z. Naturforsch.*, Vol. 23a, No. 2, pp. 242–246.
- Henschke, M. & Pfennig, A. (1999). Mass transfer enhancement in single drop extraction experiments. *AIChE J.*, Vol. 45, No. 10, pp. 2079–2084.
- Kostarev, K.G. & Pshenichnikov, A.F. (2004). Gravitational convection of a liquid mixture in a horizontal cylindrical gap at moderate Grasshoff numbers. *Cosmic research*, Vol. 42, No. 2, pp. 115–122.
- Kostarev, K.G. (2005). The study of the extraction of surface-active component of a binary liquid from model ("cylindrical") droplets. *Colloid J.*, Vol. 67, No. 3, pp. 357–362.
- Kostarev, K.G.; Levto, V.L.; Romanov, V.V.; Shmyrov, A.V.; Zuev, A.L. & Viviani, A. (2007). Experimental investigation of mass transfer in fluid systems in microgravity conditions. *Proceedings of 58th Int. Astronautical Congress*, Hyderabad, India, 2007. Paper № IAC-2007-A2.4.06. 10 p.
- Kostarev, K.G.; Levto, V.L.; Romanov, V.V.; Shmyrov, A.V. & Viviani, A. (2010). Experimental study of surfactant transfer in fluid systems in microgravity conditions. *Acta Astronautica*, Vol. 66, No. 3–4, pp. 427–433.
- Kosvintsev, S.R. & Reshetnikov, D.G. (2001). Droplet motion induced by diffusion of soluble surfactant to the external medium: experiment. *Colloid J.*, Vol. 63, No. 3, pp. 318–325.
- Lewis, J.B. & Pratt, H.R.C. (1953). Instabilities induced by mass transfer and deformable fluid interfaces. *Nature*, Vol. 171, pp. 1155–1161.
- Myshkis, A.D.; Babskii, V.G.; Kopachevskii, N.D.; Slobozhanin, L.A. & Tyuptsov, A.D. (1987). *Low-Gravity Fluid Mechanics*, Springer, the Netherlands.
- Subramanian, R.S. & Balasubramaniam, R. (2001). *The motion of bubbles and drops in reduced gravity*, Cambridge University Press, Cambridge, UK.
- Waheed, M.; Henschke, M. & Pfennig, A. (2002). Mass transfer by free and forced convection from single spherical liquid drops. *J. of Heat and Mass Transfer*, Vol. 45, No. 22, pp. 4507–4514.
- Wegener, M.; Grunig, J.; Stuber, J. & Paschedag, A.R. (2007). Transient rise velocity and mass transfer of a single drop with interfacial instabilities – experimental investigations. *Chemical Engineering Science*, Vol. 62, No. 11, pp. 2967–2978.
- Wegener, M.; Fevre, M.; Paschedag, A.R. & Kraume, M. (2009a). Impact of Marangoni instabilities on the fluid dynamic behaviour of organic droplets. *J. of Heat and Mass Transfer*, Vol. 52, No. 11–12, pp. 2543–2551.
- Wegener, M.; Paschedag, A.R. & Kraume, M. (2009b). Mass transfer enhancement through Marangoni instabilities during single drop formation. *J. of Heat and Mass Transfer*, Vol. 52, No. 11–12, pp. 2673–2677.
- Zuev, A.L. & Kostarev, K.G. (2006). Oscillation of a convective flow round the air bubble in a vertically stratified solution of a surfactant. *J. Experimental and Theoretical Physics*, Vol. 130, No. 2, pp. 363–370.



Mass Transfer in Multiphase Systems and its Applications

Edited by Prof. Mohamed El-Amin

ISBN 978-953-307-215-9

Hard cover, 780 pages

Publisher InTech

Published online 11, February, 2011

Published in print edition February, 2011

This book covers a number of developing topics in mass transfer processes in multiphase systems for a variety of applications. The book effectively blends theoretical, numerical, modeling and experimental aspects of mass transfer in multiphase systems that are usually encountered in many research areas such as chemical, reactor, environmental and petroleum engineering. From biological and chemical reactors to paper and wood industry and all the way to thin film, the 31 chapters of this book serve as an important reference for any researcher or engineer working in the field of mass transfer and related topics.

How to reference

In order to correctly reference this scholarly work, feel free to copy and paste the following:

Konstantin Kostarev, Andrew Shmyrov, Andrew Zuev and Antonio Viviani (2011). Surfactant Transfer in Multiphase Liquid Systems under Conditions of Weak Gravitational Convection, Mass Transfer in Multiphase Systems and its Applications, Prof. Mohamed El-Amin (Ed.), ISBN: 978-953-307-215-9, InTech, Available from: <http://www.intechopen.com/books/mass-transfer-in-multiphase-systems-and-its-applications/surfactant-transfer-in-multiphase-liquid-systems-under-conditions-of-weak-gravitational-convection>

INTeCH
open science | open minds

InTech Europe

University Campus STeP Ri
Slavka Krautzeka 83/A
51000 Rijeka, Croatia
Phone: +385 (51) 770 447
Fax: +385 (51) 686 166
www.intechopen.com

InTech China

Unit 405, Office Block, Hotel Equatorial Shanghai
No.65, Yan An Road (West), Shanghai, 200040, China
中国上海市延安西路65号上海国际贵都大饭店办公楼405单元
Phone: +86-21-62489820
Fax: +86-21-62489821

© 2011 The Author(s). Licensee IntechOpen. This chapter is distributed under the terms of the [Creative Commons Attribution-NonCommercial-ShareAlike-3.0 License](https://creativecommons.org/licenses/by-nc-sa/3.0/), which permits use, distribution and reproduction for non-commercial purposes, provided the original is properly cited and derivative works building on this content are distributed under the same license.

IntechOpen

IntechOpen